Journal of Applied Engineering Mathematics

Volume 12, December 2025

A Dynamic Mooring Line Model from the Wave Equation

Weston Pace

Mechanical Engineering Department
Brigham Young University
Provo, Utah 84602
wpace03@byu.edu

Abstract

As wind energy has become a popular option to propel the renewable energy industry forward, it is clear we must move offshore to obtain the most potential energy. Wind resources are superior in the ocean, and farms can be placed in locations which won't create public disturbances. However, offshore wind farms bring about new challenges not experienced onshore. Some of these include hydrodynamic loadings on the wind turbine system, energy transmission from the sea back to the grid, and innovating the floating offshore wind turbine (FOWT) design. Mooring lines are a critical design component of the FOWT and provide stability to the system under loading. In this paper, we will solve the wave equation in one-dimension to model how FOWT motion propagates through the mooring line. Following this, results of a simple simulation will be presented. In conclusion, we will discuss weaknesses of this model and possible improvements to increase its robustness.

Nomenclature

FOWT	Floating Offshore Wind Turbine
ρ	Air Density (kg/m^3)
A	Wind Turbine Swept Area (m^2)
V	Wind Turbine Inflow Velocity (m/s)
C_p	Turbine Coefficient of Power
P	Turbine Power (W)
u	Horizontal Position of Mooring Line
x	Vertical Position of Mooring Line
w	Wave Speed Coefficient (m/s)
t	Time (s)
γ	Damping Coefficient (kg/s)
ϵ	Solution Lower Bound
L	Solution Upper Bound
$f_L(t)$	Position Boundary Condition at L
$u_0(x)$	Mooring Line Initial Shape
$u_1(x)$	Mooring Line Initial Velocities
L_{SL}	Sturm-Louisville Linear Operator
λ	Eigenvalues of Sturm-Louisville Problem
J_0	Bessel Function of the First Kind, Order Zero
Y_0	Bessel Function of the Second Kind, Order Zero
y_n	Eigenfunctions of Sturm-Louisville Problem
$\mathcal{F}$	Finite Fourier Transform
$\bar{u}$	Fourier Transform of u
$\mathcal{L}$	Laplace Transform
U	Laplace Transform of $\bar{u}$
s	Laplace Variable
$*$	Convolution Operator
$\|\|y\|\|^2$	Squared Norm of Eigenfunction

Introduction

Wind energy is becoming a legitimate source of energy as we work towards reducing fossil fuel consumption. As of 2023, 5% of the worlds electricity supply comes from wind [1]. In some places, wind energy has even contributed a larger impact on power generation. In Denmark, on average, 50% of its electricity has been produced using wind, and Germany reached 30% from wind in the first half of 2020 [1]. As more and more countries move towards developing their wind energy industries, it has become apparent wind resources on land are limited, and moving wind farms offshore is an attractive solution to this problem. On one hand, the offshore wind resource is more predictable and stronger compared to onshore. While on land, things like trees, hills, or buildings affect the inflow boundary layer, these problems don't appear offshore. Furthermore, larger turbines can be installed offshore.

$$P = \frac{1}{2}\rho A V^3 C_p \tag{1}$$

Additionally, wind speeds increase by 20% every 32 feet [2], meaning a taller turbine will have access to better wind. Though some locations allow turbines to be placed in shallower waters, up to 60 meters in depth [3], most of the desired resources are located in deeper waters. At these depths, turbines have no way to be fixed to the ocean floor in traditional ways; instead, a floating structure is used to keep the turbine above the water level. To limit motion induced from hydrodynamic and aerodynamic forces, mooring lines are connected to the ocean floor.

These mooring systems are complex and critical to the longevity and safety of this system. Due to the nature of a FOWT, six-degrees of freedom can be excited. This results in noticeable motion of the FOWT, which will inevitably propagate through the mooring lines. In this study, we will model the mooring line using the wave equation in one-dimension. To match the effect of a moving turbine, we will induce periodic motion onto one of the boundary conditions. A simulation illustrating the dynamics of the mooring line will then be presented.

Figure 1: Examples of FOWT systems (adapted from Joshua Bauer, NREL [4]).

Methods

The governing equation of the mooring line will be modeled using the following form of the wave equation:

$$\frac{\delta}{\delta x}\left(x\frac{\delta u}{\delta x}\right) = \frac{1}{w^2}\frac{\delta^2 u}{\delta t^2} + 2\gamma^2\frac{\delta u}{\delta t} \tag{2}$$

$$\begin{aligned} &\epsilon < x < L, && t > 0, \\ &u(\epsilon, t) = 0, && u(L, t) = f_L(t), \\ &u(x, 0) = u_0(x), && u_t(x, 0) = u_1(x) = 0. \end{aligned}$$

This equation should sufficiently model how motion from the turbine propagates through the line. Additionally, the damping term will capture how energy in the line is lost due to viscous effects in the water.

The reason our solution ranges from $\epsilon \to L$ and not $0 \to L$ is because the differential equation will be solved using Bessel equations. However, at $x = 0$, one of our Bessel functions would be undefined. In order to enforce a stationary boundary at one end and a moving boundary at the other, we cannot start at zero.

We must first solve the governing equation's Sturm-Louisville problem. In the Sturm-Louisville solution, we will substitute y for u in order to avoid confusion between the eigenvalue solution and the final wave solution.

$$L_{SL} \cdot y = \frac{\delta}{\delta x}\left(x\frac{\delta y}{\delta x}\right) \tag{3}$$

We can write equation (3) as an eigenvalue problem and solve for y. Because solutions only exist for positive eigenvalues, we will also say $\lambda = -\mu^2$.

$$\frac{\delta}{\delta x}\left(x\frac{\delta y}{\delta x}\right) = \lambda y \tag{4}$$

$$y'' + \frac{1}{x}y' + \frac{\mu^2}{x}y = 0 \tag{5}$$

$$y = C_1 J_0\left(2\mu\sqrt{x}\right) + C_2 Y_0\left(2\mu\sqrt{x}\right) \tag{6}$$

Because our wave solution has position dependent boundary conditions, the Sturm-Louisville solution must have the homogeneous Dirichlet boundary condition at each end.

$$C_1 J_0\left(2\mu\sqrt{\epsilon}\right) + C_2 Y_0\left(2\mu\sqrt{\epsilon}\right) = 0 \tag{7}$$

$$C_1 J_0\left(2\mu\sqrt{L}\right) + C_2 Y_0\left(2\mu\sqrt{L}\right) = 0 \tag{8}$$

Combining equation (7) and (8) and picking an arbitrary value for one of the constants allows us to solve for our eigenvalues and eigenfunctions over $n = 0, 1, 2, ...$:

$$-\frac{Y_0\left(2\mu_n\sqrt{\epsilon}\right)}{J_0\left(2\mu_n\sqrt{\epsilon}\right)} J_0\left(2\mu_n\sqrt{L}\right) + Y_0\left(2\mu_n\sqrt{L}\right) = 0 \tag{9}$$

$$y_n = -\frac{Y_0\left(2\mu_n\sqrt{\epsilon}\right)}{J_0\left(2\mu_n\sqrt{\epsilon}\right)} J_0\left(2\mu_n\sqrt{x}\right) + Y_0\left(2\mu_n\sqrt{x}\right) \tag{10}$$

We now perform a finite Fourier transform on our differential operator:

$$\mathcal{F}\left(\frac{\delta}{\delta x}\left(x\frac{\delta u}{\delta x}\right)\right) = \int_{\epsilon}^{L}\left(\frac{\delta}{\delta x}\left(x\frac{\delta u}{\delta x}\right)\right) y_n(x)dx \tag{11}$$

Solving this integral gives us the following transform:

$$\mathcal{F}\left(\frac{\delta}{\delta x}\left(x\frac{\delta u}{\delta x}\right)\right) = -Lf_L(t)y_n'(L) - \mu_n^2\bar{u}_n \tag{12}$$

We then substitute the finite Fourier transform and $\bar{u}_n$ into equation (2).

$$-Lf_L(t)y_n'(L) - \mu_n^2\bar{u}_n = \frac{1}{w^2}\frac{\delta^2\bar{u}_n}{\delta t^2} + 2\gamma^2\frac{\delta\bar{u}_n}{\delta t} \tag{13}$$

Then perform the Laplace transform of equation (13).

$$\begin{aligned}-w^2\mu_n^2U_n - w^2L\mathcal{L}\{f_L(t)\}y_n'(L) = s^2U_n - \\ s\bar{u}_{n,0} - \bar{u}_{n,1} + 2\gamma^2w^2sU_n - 2\gamma^2w^2\bar{u}_{n,0}\end{aligned} \tag{14}$$

$$\bar{u}_{n,0} = \int_{\epsilon}^{L} u_0(x)y_n(x)dx \tag{15}$$

$$\bar{u}_{n,1} = \int_{\epsilon}^{L} u_1(x)y_n(x)dx = 0 \tag{16}$$

Realizing $\bar{u}_{n,1}$ is zero and performing the inverse Laplace transform on U_n, we obtain a solution for $\bar{u}_n$.

$$g(t) = e^{-\gamma^2w^2t}\sin\left(wt\sqrt{\mu_n^2 - \gamma^4w^2}\right) \tag{17}$$

$$z(t) = e^{-\gamma^2w^2t}\cos\left(wt\sqrt{\mu_n^2 - \gamma^4w^2}\right) \tag{18}$$

$$\begin{aligned}\bar{u}_n(t) = -\frac{wLy_n'(L)}{\sqrt{\mu_n^2 - \gamma^4w^2}}f_L(t) * g(t) + \\ \bar{u}_{n,0}\left(z(t) - \gamma^2w^2g(t)\right) + 2\gamma^2w^2g(t)\bar{u}_{n,0}\end{aligned} \tag{19}$$

By performing the inverse Fourier transform, we find the solution to the wave equation:

$$u(x,t) = \sum_{n=0}^{\infty}\bar{u}_n(t)\frac{y_n(x)}{||y_n||^2} \tag{20}$$

Results

To test our model, we performed a simple simulation using the following conditions:

$$\begin{aligned}&L = 1, \qquad \epsilon = 10^{-6}, \\ &f_L(t) = 1 + 0.05\sin(2\pi\cdot 0.1t), \\ &u(x,0) = 0.618\,\cosh^{-1}\left(\frac{x + (0.618 - \epsilon)}{0.618}\right)\end{aligned}$$

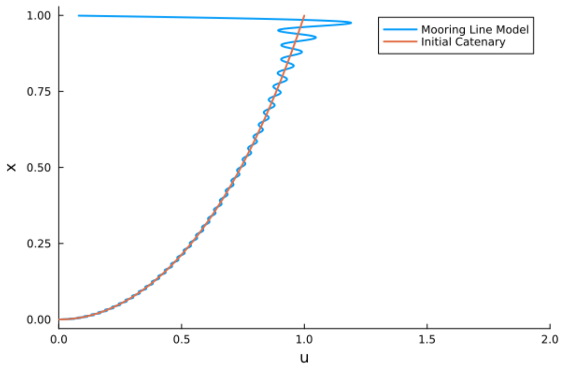

(a) Initial state

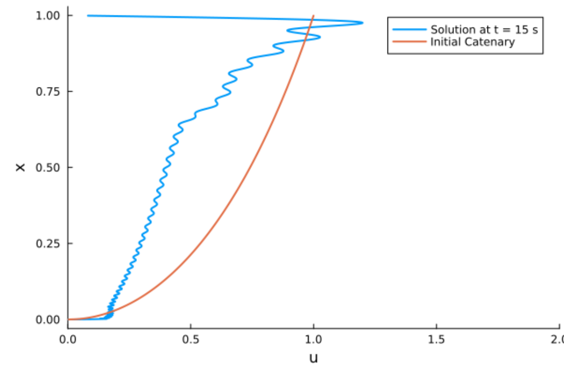

(b) 15 seconds

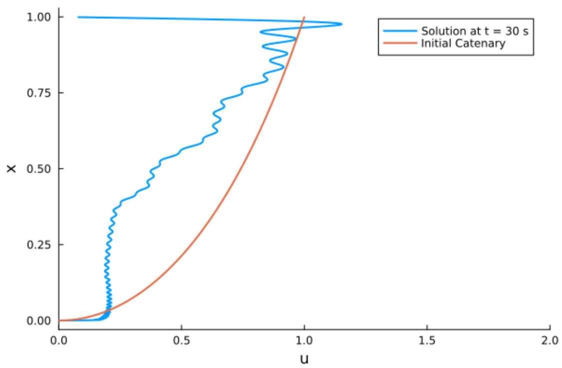

(c) 30 seconds

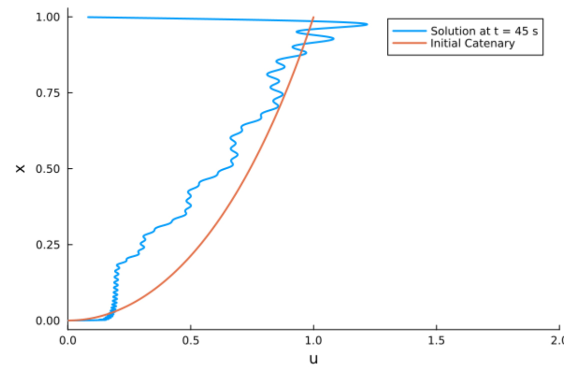

(d) 45 seconds

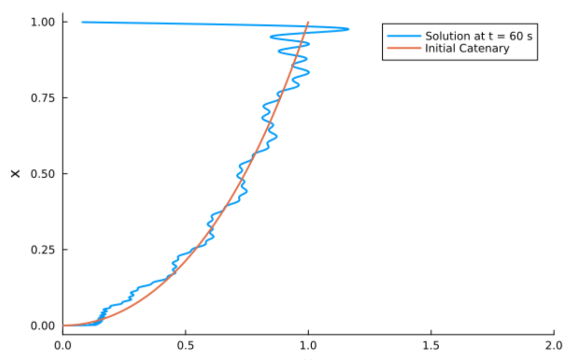

(e) 60 seconds

Figure 2: State of the mooring line simulation at several time steps compared to the initial catenary shape.

Although mooring lines are large structures extending down to depths of 1000 meters [5], we will scale our simulation to a domain length of 1 meter to save computational costs. Because a mooring line acts as a catenary at rest, we will describe the initial shape of the mooring line using the catenary equation starting at position $(0, \epsilon)$ and ending at $(1, 1)$. Finally, $f_L(t)$ was picked to simulate a floating turbine surging back and forth from a mean position of $u = 1$.

Deciding on values of γ and w are difficult because they are dependent on the the environment and properties of the mooring line. For this simulation, arbitrary values of γ and w were chosen based on assumptions of the mooring line problem. A mooring line acts underwater, so viscous effects strongly damp motion. This led us to pick a larger coefficient of $\gamma = 6$. We can get an estimate of what w should equal using equation (21), which shows us the wave propagation speed is the quotient of the tension in the line and the mass per unit length. With buoyancy reducing tension, design limits keeping tension low for fatigue life, and a relatively high line density, w is relatively small. In this test, we set $w = 0.025$.

$$w = \sqrt{\frac{T}{\rho}} \tag{21}$$

Conclusions

The results show our mooring line model does a satisfactory job demonstrating how floating turbine motion could propagate through the line. From this simulation, displacements, velocities, and accelerations could be collected at different positions along the mooring line, allowing for stresses and strains to be computed. These in turn provide valuable information about the structural integrity and lifetime of the system.

Nevertheless, this model does pose a lot of problems. To begin, underwater currents should create drag induced forces on the mooring line, but this model did not include this. Additionally, real mooring line systems are more complicated than the system used in this paper. Most mooring lines will have some length of the line resting on the ocean flooring, generating considerable amounts of friction. Furthermore, some mooring systems will place buoys underwater to relieve tension in the line, which would inevitably change the dynamics.

It is difficult to confidently say a mooring line would react as Figure 2 shows. In real life, there is likely much more damping in the system from fluid drag and friction, resulting in less wave excitation. However, with proper coefficient tuning and the addition of more realistic forces, we believe this model could better simulate mooring dynamics. The next step of this study is to find experimental data of a mooring line under similar loading conditions and tune our model. Nonetheless, as an initial study, this is very promising, and with further development, could aid in the design of future offshore systems.

Acknowledgments

Thank you Dr. Soloviev for teaching an amazing class. I've learned so much from you, and I couldn't have written this paper without your guidance. Your love for math is contagious and inspires me to live a lifetime of learning.

References

[1] Veers P, Bottasso CL, Manuel L, Naughton J, Pao L, Paquette J, Robertson A, Robinson M, Ananthan S, Barlas T, Bianchini A. Grand challenges in the design, manufacture, and operation of future wind turbine systems. Wind Energy Science. 2023 Jul 11;8(7):1071-131.

[2] "Onshore & Offshore Wind Farms: What's the Difference?", www.honeywell.com/us/en/news/featured-stories/2023/07/onshore-offshore-wind-farms-difference. Accessed 4 Dec. 2025.

[3] Training, Maersk. "Floating vs Fixed Offshore Wind Turbines – Key Differences Explained." Maersk Training, www.maersktraining.com/news-and-insights/industry-insights-blog/floating-vs-fixed-offshore-wind-turbines-key-differences-explained. Accessed 4 Dec. 2025.

[4] Carter, Laura. "Plugging into Offshore Wind Will Power up California's Renewable Energy." National Laboratory of the Rockies, NREL, 27 May 2022, www.nrel.gov/news/detail/program/2022/plugging-into-offshore-wind-will-power-up-california.

[5] Training, Maersk. "Floating vs Fixed Offshore Wind Turbines – Key Differences Explained." Maersk Training, www.maersktraining.com/news-and-insights/industry-insights-blog/floating-vs-fixed-offshore-wind-turbines-key-differences-explained.

Accessed 4 Dec. 2025.

